**Helmholtz-Zentrum Dresden-Rossendorf (HZDR)**

# 3D-Ising critical behavior in antiperovskite-type ferromagneticlike Mn3GaN

Yuan, Y.; Liu, Y.; Xu, C.; Kang, J.; Wang, W.; Wang, Q.; Song, B.; Zhou, S.; Wang, X.;

# 3D-Ising critical behavior in antiperovskite-type ferromagnetic-like Mn$_3$GaN

Ye Yuan[1,2], Yu Liu [2,3,4,*], Chi Xu[2,8], Junjie Kang[1], Weiyun Wang[1], Qi Wang[5], Bo Song[6,7,*], Shengqiang Zhou[2], and Xinqiang Wang[1,5]

[1] Songshan Lake Materials Laboratory, Dongguan, Guangdong, 523808, People's Republic of China

[2] Helmholtz-Zentrum Dresden-Rossendorf, Institute of Ion Beam Physics and Materials Research, Bautzner Landstrasse 400, D-01328 Dresden, Germany

[3] Microsoft Quantum Materials Lab Copenhagen, 2800 Lyngby, Denmark.

[4] Center for Quantum Devices, Niels Bohr Institute, University of Copenhagen, 2100 Copenhagen, Denmark.

[5] Dongguan Institute of Optoelectronics, Peking University, Dongguan, 523808, Guangdong, China

[6] Department of Physics, Harbin Institute of Technology, Harbin 150001, China

[7] National Key Laboratory of Science and Technology on Advanced Composites in Special Environments, Harbin Institute of Technology, Harbin 150001, China

[8] Institute for Integrative Nanosciences, Institute for Solid State and Materials Research (IFW Dresden), Helmholtzstrasse 20, Dresden, 01069, Germany

## Abstract:

In this work, a systematic investigation on magnetic critical behavior is performed for the first time on an antiperovskite-type Mn$_3$GaN which is prepared by intentionally modifying stoichiometry. According to the XRD results, the antiperovskite-structure is well preserved, even though all lattice parameters shrink upon reducing Ga and N content down to sixty percent. The sample exhibits a ferromagnetic-like feature with a Curie temperature ($T_C$) of 394 K rather than frustrated behavior in stoichiometric Mn$_3$GaN. Most importantly, the modified Arrot plots, Kouvel-Fisher plots as well as critical isotherm method self-consistently co-confirm the critical exponents of $\beta = 0.33$, $\gamma = 1.23$ and $\delta = 4.7$, unambiguously indicating that the critical behavior well follows the 3D-Ising model around the $T_C$.

Responding author: yu.liu@nbi.ku.dk
songbo@hit.edu.cn

# I. INTRODUCTION

The modification of magnetic structure in anti- ($A_3BC$) / perovskite-type ($ABC_3$) materials has attracted great interest due to a variety of intriguing phenomena and potential for application[1], e.g. giant barocaloric effect[2], negative thermal expansion[3, 4] as well as magnetostriction [5]. Particularly, for anti-perovskite $Mn_3AX$ materials, the manipulation of magneto-structure is of great importance for fundamental research as well as its application expansion. It is well known that, in perovskite materials, the magnetic structure is mainly dominated by the distortion of $BC_3$ octahedron which is impacted by the size of A site atom. For instance, upon gradually replacing yttrium with larger lanthanum atom in $YTiO_3$, the introduced $GdFeO_3$-type distortion drives the system into ferromagnetic (FM) from antiferromagnetic (AFM) order[6]. However, anti-perovskite type materials e.g. above mentioned $Mn_3AX$, exhibit a more complicated case: an AFM interaction [7], $J_1 < 0$, is present between nearest-neighbor atoms, while the next-nearest-neighbor magnetic interaction is FM ($J_2 > 0$)[8]. As a result, $Mn_6X$ octahedron presents a three-dimensional geometrical frustrated behavior[7], leaving a path for modulating magneto-structure through tuning the competition between FM and AFM interaction. According to the study by Takenaka *et al*., a few percent of Fe dopants at Mn sites in $Mn_3GaN$ could cause an AFM to FM phase transition[9], and an similar phenomenon is observed in carbon doped samples[10, 11]. Conclusively, the above-mentioned AFM-FM is modulated by breaking frustrated state through playing competition between $J_1$ and $J_2$, therefore offering a fruitful playground to investigate the magneto-structure in such a frustrated system.

Actually, the way of magnetic coupling always significantly impacts on the magnetic critical behavior at the region of Curie temperature ($T_C$) e.g. a 3D-Heisenburg model is always prevailing in ferromagnet with pure positive $J$ from three dimensions[12-14], while the recently attractive mono-layered 2D ferromagnet with only positive $J$ in the plane only presents 2D Ising critical feature[15]. Thus, it is a fancy topic which is worth exploring that how to describe the magnetic critical behavior in such "tuned" frustrated system with a complex competed $J$.

In the present study, we obtain a ferromagnetic-like $Mn_3GaN$ which is deviated from stoichiometry during the preparation. The X-ray diffraction results verify the preservation of anti-perovskite crystal structure, excluding the assumption that the observed ferromagnetic-like behavior is caused from the Mn-rich second phase induced by spinodal decomposition. According to the modified Arrot plots, Kouvel-Fisher plots and critical isotherm method, critical exponents of $\beta = 0.33$, $\gamma = 1.23$ and $\delta = 4.7$ are well fitted-obtained at the Curie temperature of around 394 K, well obeying the critical 3D-Ising model.

# II. EXPERIMENTAL

The preparation of the explored sample has been discussed in our previous work Ref. 16. Conventional X-ray diffraction (XRD) measurements were performed using a Rigaku D/max 2500 diffractometer with Cu Ka radiation ($\lambda = 1.5418$ Å) at room temperature, operated at 50 kV and 45 mA. Isothermal $M(H)$ data were recorded with a commercial SQUID magnetometer (MPMS Quantum Design) after zero field cooling from 400 K. After each completed data set,

the field was oscillated to zero and then the sample was heated up to 400 K before the next cycle start. For the temperature dependent magnetization measurements, the temperature was carefully increased at a rate of 0.5 K/min.

## III. RESULTS AND DISCUSSION

Figure 1 displays the XRD spectra of our $Mn_3Ga_{0.6}N_{0.6}$ together with a $Mn_3GaN$ for a reference. As shown in Fig. 1(a), both $Mn_3GaN$ and $Mn_3Ga_{0.6}N_{0.6}$ present several diffraction peaks of (110), (111), (200), (220), (311) and (222), indicating their polycrystalline nature of the cubic anti-perovskite structure. Additionally, two tiny peaks of MnO which are not negligible appear in both samples, indicating that a small amount of MnO are formatted probably during the sinter process. Actually, MnO is paramagnetic (PM), and when compared with the main antiperovskite phase its tiny mount can be ignored to influence our analysis. Interestingly, all peaks of $Mn_3Ga_{0.6}N_{0.6}$ shift to higher angle side, which suggests the reduction of lattice parameters, and such result is fully expected in nonstoichiometric sample due to the vacancy caused lattice distortion. For instance, the diffraction angle of (220) planes increases from 33.94° to 34.45°, which means that the lattice parameter of (220) planes accordingly declines from 3.90 to 3.85 Å calculated by the Bragg equation. Meanwhile, the two peaks of MnO stay constantly in $Mn_3Ga_{0.6}N_{0.6}$, which perfectly excludes the possibility of measurement error induced peak shifting.

For the ferromagnetic-paramagnetic (FM-PM) phase transition, the critical behaviour at around $T_C$ is described by a series of interrelated critical exponents according to the Landau theory [17]. Near the vicinity of phase transition point, the divergence of correlation length is defined as $\xi = \xi_0|(T-T_c)/T_c|^{-\gamma}$, causing universal scaling laws for the spontaneous magnetization $M_s$ and the inverse initial magnetic susceptibility $\chi_0^{-1}$. The $\beta$, $\gamma$, and $\delta$ are employed to characterize a set of magnetic behaviours including the $M_s$ below $T_c$, the $\chi_0^{-1}$ above $T_C$, as well as the $M(H)$ at $T_C$, respectively. Accordingly, at the temperature range around $T_C$, mathematical definitions of above-mentioned three exponents for magnetization are described as:

$$M_S(T) = M_0(-\varepsilon)^\beta, \quad \varepsilon < 0, T < T_C, \tag{1}$$

$$\chi_0^{-1}(T) = \left(\frac{h_0}{m_0}\right)\varepsilon^\gamma, \quad \varepsilon > 0, T > T_C, \tag{2}$$

$$M = DH^{1/\delta}, \quad \varepsilon = 0, T = T_C, \tag{3}$$

where $\varepsilon = (T-T_C)/T_C$ is the reduced temperature, and $M_0$, $h_0/m_0$, and $D$ are critical amplitudes[18]. In addition, by using scaling hypothesis, the magnetic equation of state is described as:

$$M(H, \varepsilon) = \varepsilon^\beta f_\pm(H/\varepsilon^{\beta+\gamma}) \tag{4}$$

where $f_+$ and $f_-$ are regular analytic functions for $T > T_C$ and $T < T_C$, respectively.

In order to clarify the nature of the PM-FM transition, we measured the isothermal magnetic field dependent magnetization $M(H)$ curves of $Mn_3Ga_{0.6}N_{0.6}$ at selected temperatures from 376 to 400 K and applied magnetic fields up to 50 kOe. The gapped temperature $\Delta T$ is set as 1 K.

For all $M(H)$ measurements, the sample was cooled down from 400 K under a zero field after stabilizing at 400 K for 10 mins. Then the initial magnetization was recorded upon gradually increasing magnetic field till 50 kOe. To explore the critical exponents of the transition, modified Arrot Plots of ($H/M$) dependent $M$ herein is performed by the Arrot-Noakes equation [19]:

$$(H/M)^{1/\gamma} = a\varepsilon + bM^{1/\beta} \tag{5}$$

where $\varepsilon = (T\text{-}T_C) / T_C$ is the reduced temperature which is the same as in Eq. (2), and $a$ and $b$ are constants. According to the Landau mean-field description, the Eq. (5) degenerates to a standard Arrot Plot in which the critical exponents $\gamma$ and $\beta$ are 1 and 0.5, respectively [20]. As a result, an ideal mean-field model described system constitutes a set of parallel straight lines, and the isotherm at the Curie temperature pass the origin [20]. As shown in Figure 2(b), the $Mn_3Ga_{0.6}N_{0.6}$ just presents a set of quasi-straight lines, and their positive slope indicates a second-order nature of PM-FM transition according to the Banerjee criterion[21]. However, a slightly up-convex of mean-field Arrot-curves suggests that the system can not be treated as an ideal mean-field model. To further explore its critical essence, two other three-dimensional (3D) models are presented to make a comparison: 3D Heisenberg model with $\gamma = 1.436$ and $\beta = 0.378$, and 3D Ising model with $\gamma = 1.230$ and $\beta = 0.330$ [22]. As shown in Fig. 2(c), the modified Arrot-plotted curves with Heisenberg critical values are obviously down-concave, indicating that the Heisenberg model is not satisfied to describe the phenomenon. However, the 3D Ising model provides an outstanding linear fitting, definitely confirming the signature of 3D Ising type transition. Meanwhile, it is worth noting that the Curie temperature of 394 K is meanwhile determined, in which the modified straight curve directly passes the origin.

To further distinguishingly confirm the critical model from Mean-field model and 3D Ising model, a rigorous interactive way is used[23]: According to Eqs. (1) and (2), the results of spontaneous magnetization $M_S(T)$ and $\chi_0^{-1}$ could be fitted by the linear extrapolation from high field region to the intercepts with the axis $M^{1/\beta}$ and $(H/M)^{1/\gamma}$, respectively, therefore a set of fitting values of $\beta$ and $\gamma$ are obtained. As shown in Fig. 3a, two solid curves nicely fit the temperature dependent $M_S(T)$ and $\chi_0(T)$ results both, accordingly two critical exponents $\beta = 0.330$ with $T_C = 394.2$ K, and $\gamma = 1.241$ with $T_C = 394.2$ K, are obtained. Such values again pronounce the dominance of 3D Ising model. To further cross-check the critical exponents deduced from our current-obtained temperature dependent magnetization results, an alternative method named Kouvel-Fisher plots is used, and its mathematical description is as below [24]:

$$\frac{M_S(T)}{dM_S/dT} = \frac{T-T_C}{\beta}, \tag{6}$$

$$\frac{\chi_0^{-1}(T)}{dx_0^{-1}(T)/dT} = \frac{T-T_C}{\gamma} \tag{7}$$

Therefore, according to Eqs. (6) and (7), $M_S(T) / [dM_S(T) / dT]$ and $\chi_0^{-1}(T) / [d\chi_0^{-1}(T) / dT]$ are respectively as linear functions of temperature with slopes $1/\beta$ and $1/\gamma$. The fitting results are given in Fig. 3(b), claiming the fitting values for $\beta = 0.340$ with $T_C = 394.2$ K, and $\gamma = 1.244$ with $T_C = 394.0$ K, respectively. As expected, the Kouvel-Fisher fitted values are highly consistent with former calculated critical components and $T_C$ from modified Arrot-Noakes plots, which cross-confirms the description of 3D Ising model.

To reveal third critical component δ which appears in Eq. (3), the isothermal magnetization $M(H)$ result at the critical temperature of 394 K together with a double-logarithmic plot is shown in Figure 4. According to the Eq. (3), the δ is calculated as 4.727 by the slope of linear double-logarithmic plot shown in the inset of Figure 4. Alternatively, the Windom scaling law works:

$$\delta = 1 + \frac{\gamma}{\beta} \tag{8}$$

where the $\beta$ and $\gamma$ are obtained from modified Arrot plots or Kouvel-Fisher fitting. Accordingly, the δ is calculated as 4.727, which is exactly the same as the value deduced from Eq. (3).

It is worth noting that the obtained critical exponents and $T_C$ are verified reliably by a scaling analysis. According to Eq. (4), the scaling equation displays that M(H, ε) vs. H / $\varepsilon^{\beta+\gamma}$ should lead to two different branches: $T > T_C$ and $T < T_C$. The isothermal magnetization curves around $T_C$ = 394 K are plotted in Figure 5 with an aid of critical exponents $\beta = 0.33$, $\gamma = 1.23$. As a result, all plots evolve into two independent sets of curves as expected: $T > T_C$ and $T < T_C$, indicating that the reliability of the obtained critical exponents. For a comparison, the obtained critical exponents of $Mn_3Ga_{0.6}N_{0.6}$ as well as that from different theoretical values are listed in Table I.

Table I. Comparison of critical exponents of $Mn_3Ga_{0.6}N_{0.6}$ with different theoretical models.

| Composition | Technique | B | γ | δ | References |
|---|---|---|---|---|---|
| $Mn_3GaN$ | Modified Arrot Plots | 0.330±0.006 | 1.23±0.01 | 4.7±0.1[cal] | This work |
| $Mn_3GaN$ | Kouvel-Fisher Method | 0.330±0.002 | 1.24±0.01 | 4.7±0.1[cal] | This work |
| Mean-field | Theory | 0.5 | 1.0 | 3.0 | [17] |
| 3D-Heisenberg | Theory | 0.365 | 1.386 | 4.8 | [17] |
| 3D-Ising | Theory | 0.325 | 1.24 | 4.82 | [17] |
| 2D-Ising | Theory | 0.125 | 1.75 | 15 | [17] |
| 3D-XY | Theory | 0.345 | 1.316 | 4.81 | [17] |

## IV. CONCLUSION

In summary, we report systematical investigations on critical behavior of ferromagnetic-like antiperovskite-type $Mn_3Ga_{0.6}N_{0.6}$ which is produced away from the stoichiometry. Around its $T_C$ of around 394 K, according to the modified Arrot plots, Kouvel-Fisher plots and critical isotherm method, three critical exponents, β, γ, and δ are deduced to be 0.33, 1.23 and 4.7, respectively, which are highly in agreement with the 3D Ising model. Moreover, the calculated values follow the scaling equation, again confirming the intrinsic 3D Ising essence of ferromagnetic-like $Mn_3Ga_{0.6}N_{0.6}$.

**REFERENCES**

1. Y. Tokura and N. Nagaosa, Science **288** 462-468 (2000).

2. D. Matsunami, A. Fujita, K. Takenaka and M. Kano, Nat. Mater. **14**, 73-78 (2015).

3. K. Takenaka, K. Asano, M. Misawa and H. Takagi, Appl. Phys. Lett. **92**, 011927 (2008).

4. K. Takenaka and H. Takagi, Appl. Phys. Lett. **87**, 261902 (2005).

5. K. Takenaka and H. Takagi, Appl. Phys. Lett. **94**, 131904 (2009).

6. W. Knafo, C. Meingast, A. V. Boris, P. Popovich, N. N. Kovaleva, P. Yordanov, A. Maljuk, R. K. Kremer, H. V. Lohneysen and B. Keimer, Phys. Rev. B **79**, 054431 (2009).

7. D. Tahara, Y. Motome and M. Imada, J. Phys. Soc. Jpn. **76**, 013708 (2007).

8. E. F. Bertaut, D. Fruchart, J. P. Bouchaud and R. Fruchart, Solid State Commun. **6**, 251-256 (1968).

9. K. Takenaka, T. Inagaki and H. Takagi, Appl. Phys. Lett. **95**, 132508 (2009).

10. D. B. Fruchart and E. F. Bertaut, J. Phys. Soc. Jpn. **44**, 781-791 (1978).

11. P. B. I'Heritier, D.; Fruchart, R.; Fruchart, D. , Mater. Res. Bull. **14**, 1203-1212 (1979).

12. B. Banerjee, Phys. Lett. **12**, 16 (1964).

13. Yu Liu, V. N. Ivanovski, and C. Petrovic, Phys. Rev. B **96**, 144429 (2017).

14. Yu Liu and C. Petrovic, Phys. Rev. B **97**, 014420 (2018).

15. G. C. B. Huang, E. Navarro-Moratalla, D. R. Klein, R. Cheng, K. L. Seyler, D. Zhong, E. Schmidgall, M. A. McGuire, D. H. Cobden, W. Yao, D. Xiao, P. Jarillo-Herrero, and X. D. Xu, Nature **546**, 270 (2017).

16. Q. Y. Xinghong Zhang, Tangling Gao, Yang Ren, Hui Wu, Qingzhen Huang, Jinggeng Zhao, Xianjie Wang, Ye Yuan, Chi Xu, Yongfeng Hu, James, J. Dynes, Jigang Zhou, Shengqiang Zhou, Yu Liu, and Bo Song, J. Mater. Chem. C **6**, 13336 (2018).

17. H. E. Stanley, *Introduction to Phase Transitions and Critical Phenomena (Oxford University Press, London, 1971).*

18. M. E. Fisher, Rep. Prog. Phys. **31**, 418 (1968).

19. A. Arrott and J. E. Noakes, Phys. Rev. Lett. **19**, 786 (1967).

20. A. Arrott, Phys. Rev. **108**, 1394-1396 (1957).

21. S. K. Banerjee, Phys. Lett. **12**, 16-17 (1964).

22. J. C. Leguillou and J. Zinnjustin, Phys. Rev. B **21**, 3976-3998 (1980).

23. A. K. Pramanik and A. Banerjee, Phys. Rev. B **79**, 214426 (2009).

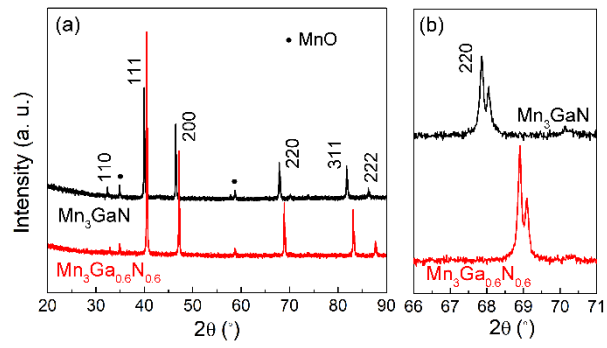24. J. S. F. Kouvel, M. E. Fisher, Phys. Rev. **136**, A1626 (1964).

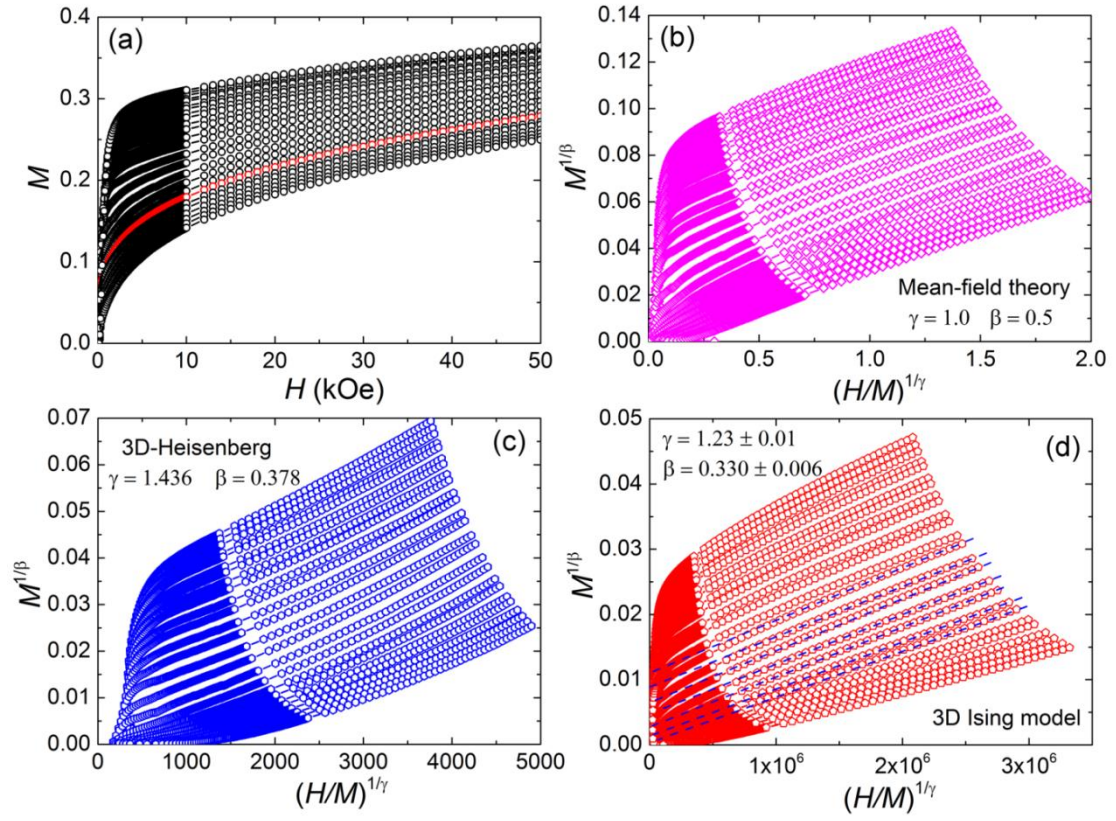Figure 1 (a) XRD spectra for samples Mn$_3$GaN and Mn$_3$Ga$_{0.6}$N$_{0.6}$ and corresponding (b) (220) diffraction peaks

Figure 2 (a) Typical initial isothermal magnetization curves from $T = 376$ to 400 K for $Mn_3Ga_{0.6}N_{0.6}$. (b-d) The isotherms plotted as $M^{1/\beta}$ vs $(H/M)^{1/\gamma}$ with a (b) 3D Heisenberg model (c) Mean-field theory model, and (d) 3D Ising model. The $\Delta T$ is selected as 1 K.
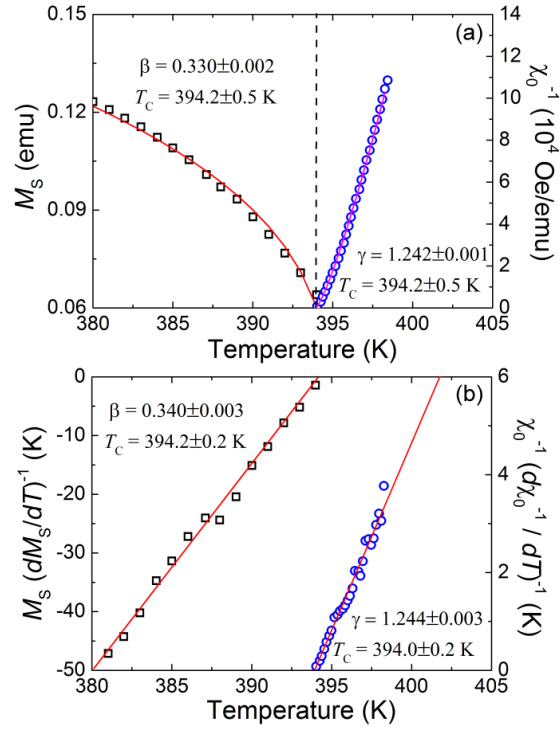
Figure 3 (a) Temperature dependence of the spontaneous magnetization $M_S$ (left) and the inverse initial susceptibility $\chi_0^{-1}$ (right) with solid fitting curves for $Mn_3Ga_{0.6}N_{0.6}$. The curves represent fits of Eqs. (1) and (2) to the data with the exponents $\beta = 0.33$ and $\gamma = 1.24$. (b) Kouvel-Fisher plots of $M_S(dM_S/dT)^{-1}$ (left) and $\chi_0^{-1}(d\chi_0^{-1}/dT)^{-1}$ (right) with solid fitting curves.
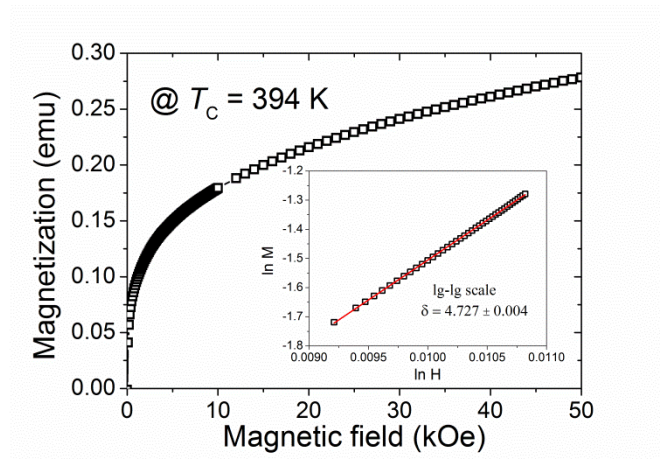
Figure 4. Isotherm $M(H)$ plot collected at $T_C = 394$ K for $Mn_3Ga_{0.6}N_{0.6}$. Inset: The same data shown in double-logarithmic plot with a solid fitting curve.
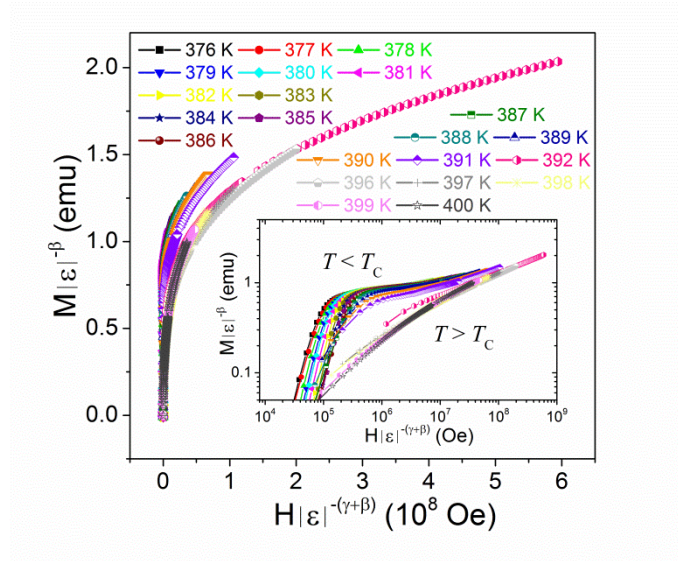
Figure 5 Scaling plots of the $M(H)$ data of $Mn_3Ga_{0.6}N_{0.6}$ for temperatures ranging from 376 K to 400 K using the values $\beta = 0.33$, $\gamma = 1.23$, and $T_C = 394$ K. The inset: Scaling plot in a double-logarithmic scale.